ANNUAL REVIEWS

Annual Review of Biochemistry

Electron Transport Across Bacterial Cell Envelopes

Joshua A.J. Burton,[1] Marcus J. Edwards,[2] David J. Richardson,[1] and Thomas A. Clarke[1]

[1]School of Biological Sciences, University of East Anglia, Norwich, United Kingdom; email: tom.clarke@uea.ac.uk

[2]School of Life Sciences, University of Essex, Colchester, United Kingdom

Annu. Rev. Biochem. 2025. 94:89–109

First published as a Review in Advance on March 17, 2025

The *Annual Review of Biochemistry* is online at biochem.annualreviews.org

https://doi.org/10.1146/annurev-biochem-052621-092202

Keywords

extracellular electron transfer, *Shewanella*, *Geobacter*, porin–cytochrome, multiheme cytochrome, protein modeling

Abstract

Extracellular electron transfer is an ancient and ubiquitous process that is used by a range of microorganisms to exchange electrons between the cell and environment. These electron transfer reactions can impact the solubility and speciation of redox-active molecules in the environment, such as metal oxides, while allowing bacteria to survive in areas of limited nutrient availability. Controlled transfer of electrons across the cell envelope requires assembly of electron transport chains that must pass through the outer membrane of Gram-negative bacteria or the S-layer of Gram-positive bacteria, but the mechanisms used by bacteria are still far from understood. Here, we review the literature surrounding characterized extracellular electron transfer pathways and use protein modeling tools to investigate novel electron transfer proteins and protein complexes. While these protein models are hypothetical, they provide new insight into features that may explain how extracellular electron transfer complexes interact with a range of different environmental substrates.

Contents

ROLE AND IMPORTANCE OF EXTRACELLULAR ELECTRON TRANSFER IN MICROBIAL METABOLISM

Extracellular electron transfer (EET) is commonly utilized by bacteria either to release electrons generated by unbalanced catabolic reactions or to import electrons for reductive anabolic processes (1–3). Use of EET influences both the metabolism of the bacterial cell and also the redox state of the environment (3), and these processes are likely to have allowed some of the earliest forms of life to proliferate through the reduction of inorganic materials (4). Today, these same fundamental reactions control the bioavailability of different metal ions within the subsurface, including iron and manganese, which are essential for plant growth (5). Current applications for EET focus around biomining and microbial fuel cells, and while biomining is a cost-effective method of extracting copper and gold from low-grade metal ores, the production of electricity from microbial fuel cells is uncompetitive compared to other renewable technologies (6). However, microbial fuel cells can also be coupled to alternative respiration streams such as desalination and wastewater treatment (7) or used in biotechnology as a means of removing excess electrons from unbalanced fermentation processes (8), resulting in more cost-effective processes. More recently, research into EET applications has focused on bioremediation, including the dissolution and precipitation of arsenic compounds in aquifers, the removal of radionuclides from contaminated groundwater, and the recovery of rare metals from electronic waste streams (9, 10). There are also potential health implications for EET processes, as many eukaryotic cells are influenced by the potential of their environment and several pathogenic bacteria have demonstrated the ability to respire using EET under anaerobic conditions (11–13).

EET is a significant challenge for most bacteria, as it requires the controlled exchange of electrons with the extracellular environment without interfering with the redox balance of the cell

or generating harmful metabolites in either the cell or the environment. This requires dedicated transporter systems that control the passage of electrons throughout the cell (1). Electrons that are released in the cytoplasm by catabolic reactions are transferred via a range of electron shuttles, such as NADH, to quinones in the cytoplasmic membrane. The reduced quinols freely diffuse across the membrane and are reoxidized by the quinol dehydrogenases on the periplasmic face of the cytoplasmic membrane. In Gram-negative bacteria, the cytoplasmic and outer membranes are separated by the periplasm, which varies in width from 10 nm to 40 nm in different EET species (14). The periplasm contains a dense matrix of peptidoglycan and protein that limits diffusion of electron carriers. Furthermore, the outer membrane represents an insulative barrier that prevents efficient electron transfer to the surface of the cell, so systems for efficient transfer of electrons across this barrier must be established (15). In Gram-positive bacteria, the reduction of extracellular substrates occurs either through the transport of the substrate through the S-layer of the cell surface and catalytic reduction on the surface of the cytoplasmic membrane (16) or through the reduction of substrates on the surface of the S-layer (17).

At the cellular surface, there exist catalytic mechanisms for facilitating direct electron exchange with the environment. For electron exchange with diffusible substrates like Fe(II) or soluble organic compounds, this reaction can occur directly at the cell surface. However, with insoluble substrates that have limited access to the cell surface, such as Fe(III) oxides, electron exchange can take place either through direct contact with electron transfer proteins protruding from the cell surface or via diffusible mediators secreted to bridge the gap between the cell and the substrate (1). To generate energy from this process, bacteria undertaking EET synthesize quinol dehydrogenases capable of abstracting both protons and electrons from the inner-membrane quinone pool into the periplasm, generating a proton gradient across the inner membrane. Because respiratory EET is a process that results in the reduction of substrates on the surface of the cell, energy is lost during these oxidative reactions, and because of this, EET as part of respiration is often described as dissimilatory respiration, as energy is lost during the reductive part of the cycle (18).

This review explores our current understanding of the known mechanisms of EET in both Gram-negative and Gram-positive bacteria, examining both experimentally derived data and recent computational models to identify key characteristics of EET within these bacterial groups and the current gaps in understanding these processes.

IDENTIFICATION OF EXTRACELLULAR ELECTRON TRANSFER

The first bacteria identified as being capable of EET were from the *Shewanellacea* and *Geobacteracea* families (19, 20); these bacteria were shown to catalyze the reduction of insoluble Fe(III) hydroxides and Mn(IV) oxides and therefore must have a mechanism for EET, although the precise details of the delivery of electrons to the mineral surface were unclear. Similar experimental evidence was obtained for both neutrophilic and acidophilic iron oxidizers grown in media using solid Fe(II) sulfide as the electron donor (21, 22). Genome sequencing of these isolated species then allowed for screening to identify novel cell envelope proteins that could allow EET. Once potential pathways of EET were identified, they required experimental validation. In early studies, the EET pathway of *Shewanella oneidensis* MR-1 was identified through deletion of the *mtr* operon (23), and in *Acidithiobacillus ferrooxidans*, an outer-membrane EET system was confirmed biochemically through identification of the Cyc2 heme protein in the outer membrane (24). The bacteria *Geobacter sulfurreducens* PCA and *Sideroxydans lithotrophicus* ES-1 were also shown to interact with insoluble iron oxides or iron sulfides, respectively. Moreover, the genomes of these bacteria contain multiple gene clusters encoding different outer-membrane protein complexes that could potentially support EET and be expressed under different environmental stresses (25–27).

The presence of unusual electron transfer complexes in the bacterial outer membrane or S-layer is not always necessary for EET. More recently several examples of EET systems have been identified that rely on the passive diffusion of mediators from reductases located on the cell membrane. For example, the Gram-negative *Pseudomonas aeruginosa* is capable of reducing phenazine, which acts as a toxin for other bacteria (28), while the Gram-positive *Listeria monocytogenes* has an extracellular flavin reductase system that uses soluble flavin as a mediator between the cell membrane and extracellular substrates (11), and *Enterococcus faecalis* is proposed to use quinol-like molecules as mediators for respiration (12). These mechanisms allow for cell survival in challenging environments where there may be substantial competition for alternative electron acceptors.

Even after identification of gene clusters that confer the ability to reduce extracellular substrates, the actual mechanism of electron transfer can still be unclear. This is because many organisms that undergo EET are poorly characterized and do not grow to significant biomass. Despite recent progress in assembling porin–cytochrome EET complexes in heterologous hosts, the formation of an assembled complex has not been fully demonstrated, and EET rates are still substantially lower than in native systems (29–31). The Cyc2 protein can be identified in membranes of *Acidithiobacillus* bacteria grown aerobically using Fe(II) as an electron donor, but the low cell densities make it hard to extract and isolate sufficient protein for analysis (32). In the laboratory, neutrophilic iron oxidizers grow slowly under microoxic conditions in a semisolid mixture of iron sulfide, making it hard to generate high cellular yields. Consequently, it has not yet been possible to generate and isolate sufficient biomass for any substantial biochemical detail to be explored on the outer membranes of iron oxidizing bacteria.

The main organism involved in studying the molecular mechanism of EET in Gram-negative bacteria has been *S. oneidensis* MR-1, originally isolated in sediments from Lake Oneida (New York, USA) (19). It is genetically tractable and easy to grow, and importantly, the EET pathway is expressed under anaerobic and microaerobic conditions, allowing for milligram quantities of the porin–cytochrome complex, known as the MtrCAB complex, to be isolated. This allowed for initial biochemical and spectroscopic analyses of the complex and its components to be undertaken. Despite these advances, the catalytic properties of porin–cytochrome complexes remained challenging to investigate: The primary function of these complexes is to transfer electrons across a membrane, so any in vitro study requires separating the catalytic redox reactions at opposite ends of the complex. This means that most electron transfer experiments lack the ability to distinguish these individual redox reactions.

BIOCHEMICAL MEASUREMENT OF EXTRACELLULAR ELECTRON TRANSFER

In vitro analysis of EET by isolated membrane protein complexes is challenging due to the need to measure directional electron transfer across the protein. One method to study EET rates in vitro is to incorporate the complex into a synthetic liposome that contains a membrane-impermeable redox-active substrate. Typically, these are formed in a solution with a concentrated redox acceptor and then separated using ultracentrifugation or chromatography. Small amounts of detergent-solubilized porin–cytochrome close to the detergent's critical micellar concentration (CMC) are added to the liposomes, and the dilution causes the porin–cytochrome complexes to spontaneously insert into the liposome (33). The complexes insert into the liposome membrane in the most thermodynamically favorable orientation, which for larger complexes means that the surface-exposed extracellular domains face outward, mimicking the orientation found in nature. Larger proteoliposomes containing more porin–cytochromes can be made by diluting both

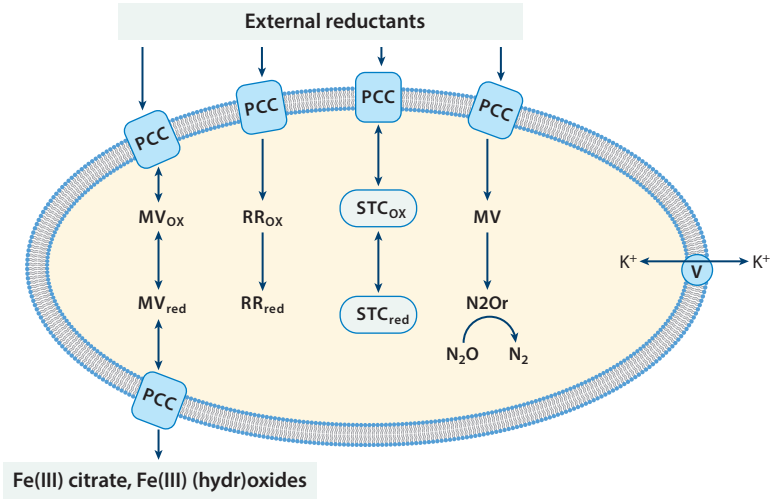

Figure 1

Proteoliposome model for studying extracellular electron transfer. PCCs are embedded within a phospholipid bilayer. Addition of an external reductant such as sodium dithionite allows for transmembrane electron transfer to internalized electron acceptors such as MV, RR, STC, and N2Or. Valinomycin is used as a potassium transporter to balance charge across both sides of the membrane. Reduced proteoliposomes can be used to reduce extracellular substrates such as soluble Fe(III) chelates or insoluble Fe(III) (hydr)oxides. Abbreviations: MV, methyl viologen; N2Or, nitrous oxide reductase; OX, oxidized; PCC, porin–cytochrome complex; red, reduced; RR, Reactive Red; STC, small tetraheme cytochrome; V, valinomycin.

detergent-solubilized proteins and lipids below the CMC, although this causes the liposome to form with the porin–cytochromes in both orientations across the lipid bilayer (34) (**Figure 1**).

Adding an external electron donor to anaerobic suspensions of these proteoliposomes allows for the rate of electrons flowing through the complex to be measured spectroscopically by monitoring changes in the ultraviolet-visible spectra corresponding to the redox state of the internalized redox dye. The MtrCAB complex of *S. oneidensis* has been studied in liposome systems using a range of internalized substrates. These include organic molecules such as methyl viologen and Reactive Red, or cytochromes such as small tetraheme cytochrome (33–35). These are reduced by the addition of an external reductant, most commonly sodium dithionite, and can then be used to monitor the catalytic properties of the MtrCAB complex by adding Fe(III) oxides or other substrates to prereduced MtrCAB proteoliposomes. The oxidation of the internalized redox molecule is monitored to determine the rate of reduction of the extracellular substrate. More recently, MtrCAB proteoliposomes have been used to demonstrate the potential for light-driven reduction of Reactive Red using MtrCAB complexed with photoactive particles including titanium oxides or carbon dots (34). It has also been possible to use MtrCAB proteoliposomes to drive internalized catalytic enzymes such as nitrous oxide reductase (36).

The porin–cytochromes of *G. sulfurreducens* PCA have also been characterized using the proteoliposome method. Heterogenic mixtures of porin–cytochrome complexes were extracted from the outer membranes of *G. sulfurreducens* grown on Fe(III) citrate. The relatively low concentrations of protein meant that little structural or spectroscopic information could be obtained. However, it was possible to show these porin–cytochrome complexes were capable of reducing both Fe(III) citrate and ferrihydrite at catalytic rates comparable to MtrCAB. These complexes remain the only other complexes experimentally shown to be capable of EET (37).

STRUCTURAL AND BIOCHEMICAL CHARACTERIZATION OF EXTRACELLULAR ELECTRON TRANSFER COMPLEXES

The MtrCAB Porin–Cytochrome Complex

The domain organization of the porin–cytochrome complex of *S. oneidensis* MR-1 was first proposed in 2009, but it was not until 2020 that the first structure of the MtrCAB complex from *Shewanella baltica* OS185 was resolved (38, 39). Currently, this is the only experimentally determined structure of a transmembrane complex capable of EET. The MtrCAB porin–cytochrome complex consists of three proteins, MtrA, MtrB, and MtrC (**Figure 2*a***). MtrA is a small, soluble decaheme cytochrome in which the hemes are tightly packed in a linear chain approximately 80 Å long. MtrA is enfolded by MtrB, a 26-strand β-barrel that wraps around MtrA in the outer membrane. The terminal hemes of the MtrB-associated MtrA are exposed to the periplasm and extracellular environment such that electron transfer can occur across the outer membrane through the chain of hemes. MtrC binds tightly to MtrA at the outer membrane surface and acts as a hub for electron transfer, allowing electrons to reach a multitude of different extracellular redox partners (**Figure 2*a***). The association between MtrC and MtrAB is extremely stable, and the functional complex can be formed by adding exogenous soluble MtrC to cells missing the *mtrC* gene, restoring the extracellular reduction of metals and flavin groups (40).

MtrAB forms the core porin–cytochrome component of the complex, and it is possible for electrons to pass across the outer membrane through MtrAB in the absence of MtrC. The hemes of MtrA are closely packed within 6 Å of each other and are capable of rapid electron transfer across the 80-Å length of MtrA (**Figure 2*b***). The rate of electron transfer between the two terminal hemes has not yet been measured, but molecular dynamic simulations predicted that electrons

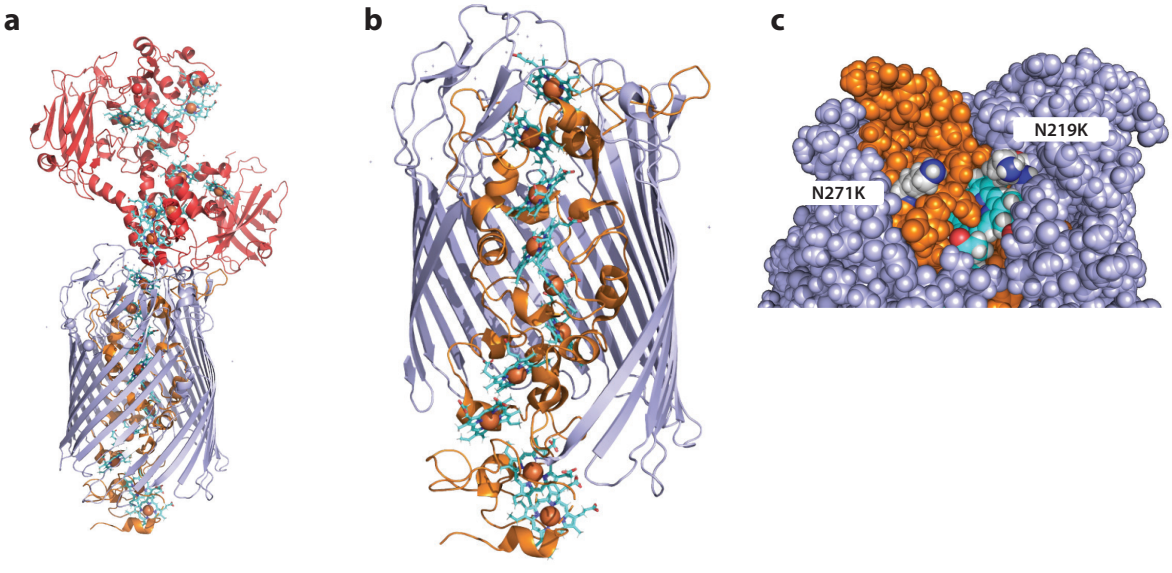

Figure 2

X-ray crystal structure of the transmembrane porin–cytochrome complex MtrCAB from *Shewanella baltica*. (*a*) Ribbon diagram of the MtrCAB complex and (*b*) cross section of the transmembrane MtrAB showing the arrangement of MtrA inside the porin. The complex consists of the decaheme MtrA (*orange*) embedded within the porin MtrB (*blue*) and the decaheme MtrC (*red*), with hemes shown in cyan. (*c*) Sphere representation of the surface of MtrB revealing the arginine-to-lysine changes at MtrA 290 and MtrB 219 that allow Fe(III) citrate respiration.

could travel through the 10-heme MtrA wire at a rate of 2×10^5 s^{-1} (41). These rates suggest that electron transfer through the membrane is limited by the exchange of electrons from redox partners on either side of the membrane (42). In the absence of MtrC, the MtrAB complex is unable to reduce insoluble iron or manganese oxides or metal chelates such as Fe(III) citrate (43). MtrA binds tightly to MtrB at the extracellular side of the lipid bilayer, but on the periplasmic side, MtrA is solvent exposed, allowing the three exposed hemes to access electron donors within the periplasm. There is little exposure of the terminal MtrA heme on the extracellular surface of the membrane, which limits reduction of small soluble metals such as Fe(III) citrate and prevents reduction of insoluble metal oxides or organic mediators such as flavins. Despite this, it is possible for the extracellularly exposed terminus of MtrAB to be modified to accelerate electron transfer to soluble substrates. In a directed evolution experiment, reduction of Fe(III) citrate was restored by the spontaneous mutation of two asparagines to lysines in MtrA and MtrB (44). Mapping these residues onto the MtrAB structure showed these amino acids were close to the surface of the MtrA C-terminal heme, thereby altering its ability to interact with soluble extracellular substrates (**Figure 2*c***).

Orthologs of the MtrAB Complex

Resolution of the MtrAB complex allowed not just the structures of MtrAB homologs from other species to be investigated but also paralogous *Shewanella* systems including the DmsEF and MtrDE EET complexes. DmsEF forms part of the outer-membrane dimethylsulfoxide reductase system in *Shewanella*, while MtrDE forms a secondary EET complex in some *Shewanella* species that has unknown function (39). These paralogs can be compared with some confidence, as the sequence identity between MtrA and MtrD or DmsE is 72% or 67%, respectively, suggesting that the MtrAB heme wire is structurally conserved.

Orthologs of MtrAB from different organisms can also be compared to gain mechanistic insight. The *mtoAB* gene cluster from *S. lithotrophicus* ES-1 has sequence homology to the *mtrAB* gene cluster and is also predicted to form a structurally similar porin–cytochrome complex that lacks the surface-exposed component. MtoA has been shown to be a decaheme *c*-type cytochrome that contains 10 bis-His-coordinated residues, and its amino acid sequence is 37% identical to MtrA (45). The product of *mtoB* has not yet been experimentally characterized, but the predicted amino acid is 23% identical to MtrB and is reported to generate a 26-strand β-barrel. Both *mtoA* and *mtoB* share a gene cluster with MtoD, a high-potential *c*-type cytochrome that is proposed to mediate electron transfer from MtoAB to proton-powered quinol reductases in the inner membrane (46). The *mto* genes have also been shown to be upregulated in the presence of the insoluble clay Fe(II)–smectite, indicating that the Mto pathway is involved in solid Fe(II) oxidation (27).

The other characterized porin–cytochrome complex is PioAB of *Rhodopseudomonas palustris* TIE-1. PioA and PioB share 8% and 22% sequence similarity with MtrA and MtrB, respectively. PioA is predicted to be a *c*-type cytochrome with 10 hemes arranged in a linear chain and forms a complex with PioB in the outer membranes of *R. palustris* TIE-1 (47). PioA is unusual in that spectroscopic analysis and sequence alignments comparing the distal ligands of MtrA and PioA show that up to three hemes of PioA may be His–Met coordinated (48). The role and impact of these His–Met-coordinated hemes in a linear electron transfer chain are not yet clear.

Fused Porin–Cytochromes

The fused porin–cytochrome Cyc2 was first identified in *Acidithiobacillus* but has also been found in other iron-oxidizing bacteria including *S. lithotrophicus* and *Mariprofundus ferrooxydans* (49, 50). This porin–cytochrome is of significant biotechnological importance as it is expressed under both

acidophilic and neutrophilic conditions where it is responsible for the uptake of electrons from soluble ferrous iron during the biological recovery of copper and gold from acidic mining waste streams and low-grade ores. The *cyc2* gene of *Acidithiobacillus* encodes for a protein that is predicted to contain both an 18-strand β-barrel and a single monoheme domain. Cyc2 is located in the outer membrane and is proposed to receive electrons from soluble Fe(II) in the acidic environment through two iron-binding sites within the porin cleft. More recently, several groups have had success with the production of recombinant Cyc2 from *Mariprofundus* (51). These initial studies have allowed the isolation of a single protein containing a high-potential heme. This provided a heme spectrum containing a Soret peak at 410 nm, a reduced Soret peak at 427, and Q-bands at 530 nm and 560 nm, away from the typical peaks of a *c*-type cytochrome (51). These experimental studies are bringing us closer to understanding the function and mechanism of action of these remarkable fused porin–cytochrome complexes.

ROLE OF CELL-SURFACE PROTEINS IN EXTRACELLULAR ELECTRON TRANSFER

Shewanella Outer-Membrane Cytochromes Involved in Extracellular Electron Transfer

For bacteria that transfer electrons to insoluble electron acceptors, such as *Shewanella* and *Geobacter*, the identified porin–cytochrome complexes to date all contain a third component that is localized to the cell surface and facilitates electron transfer from the cell envelope. Since 2011, a large range of outer-membrane cytochrome (OMC) structures have been solved through the use of techniques such as X-ray crystallography and cryo–electron microscopy (cryo-EM), and several structures have now been obtained of cell-surface reductases involved in EET.

The most extensively studied family of cell-surface cytochromes (CSCs) involved in EET are the OMCs from the *Shewanella* family. Through X-ray crystallography, the complete structures of the decaheme cytochromes MtrF, MtrC, and OmcA and the 11-heme UndA have been obtained over the last decade, and together, these proteins represent the major clades of the *Shewanella* OMCs (52–55).

The domain arrangement of the OMCs is conserved, consisting of four domains, with a split β-barrel N-terminal domain, a pentaheme domain, and a second split β-barrel domain followed by a second pentaheme or hexaheme domain (**Figure 3*a***). The four domains are arranged so that the two multiheme domains come into close contact with their hemes, forming a decaheme or undecaheme staggered-cross configuration. This results in an electron transfer pathway whereby electrons can freely move between the two domains, allowing for up to four putative ingress/egress sites. In all four structures, the hemes are low-spin hexacoordinated, with the heme iron coordinated by the porphyrin and two histidine ligands (56). The staggered-cross heme motif was also conserved, with the exception of UndA, in which the additional heme was positioned between hemes 6 and 7. Initially, the high level of symmetry and lack of high-spin hemes made it impossible to determine the orientation on the membrane surface. After resolution of the MtrCAB complex, the orientation of MtrC revealed that heme 10 was the likely egress site for electrons. This indicates that the paralog MtrF is likely to have a similar orientation, with heme 10 being the site of substrate reduction and heme 5 receiving electrons from a MtrDE porin–cytochrome complex. This orientation of MtrC/MtrF as part of a hard-wired complex on the surface of the cell is consistent with the role of OMC as a catalytic center for the reduction of a broad range of different substrates, including soluble Fe(III) chelates, flavins, insoluble metal oxides, and humic acids.

While MtrF and MtrC are part of porin–cytochrome complexes and have a defined orientation, the OmcA and UndA components appear to have a different role. OmcA and UndA do not

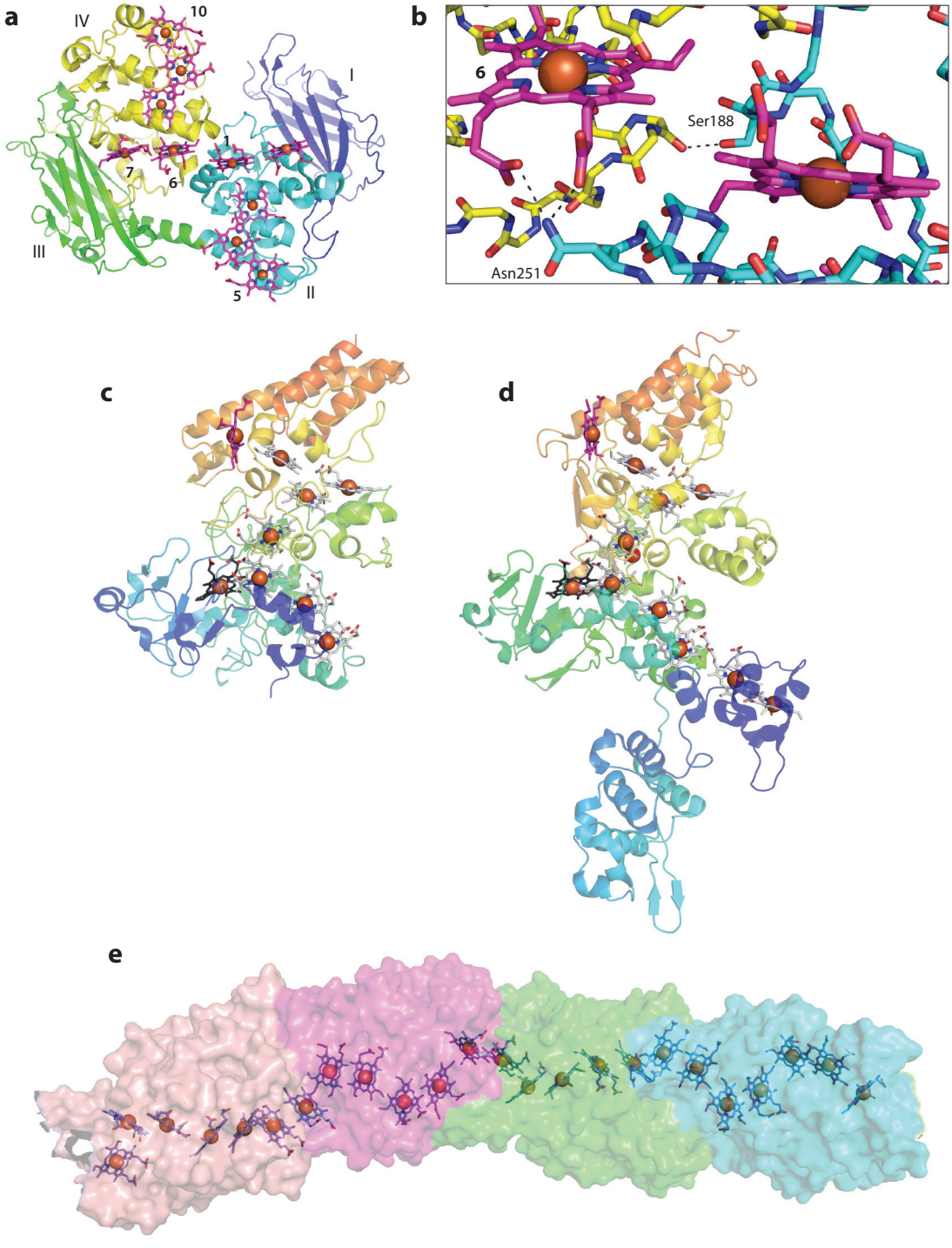

(*Caption appears on following page*)

Figure 3 (*Figure appears on preceding page*)

Structures of cell-surface cytochromes. (*a*) Crystal structure of MtrC from *Shewanella oneidensis* colored by domain [Protein Data Bank identifier (PDB ID): 4LM8]. (*b*) Hydrogen bonds located in MtrC between Asn251 and Ser188 that stabilize the interdomain configuration. (*c*) OcwA from *Thermincola potens* (PDB ID: 6I5B). (*d*) OmhA from *Carboxydothermus ferrireducens* (PDB ID: 6QVM). Structures are shown in ribbon format and colored using the red–blue spectrum from the N terminal (*red*) to the C terminal (*blue*). Hemes are shown as sticks with irons as orange spheres; bis-His-coordinated hemes are shown in cyan, His–Met-coordinated hemes are shown in purple and pentacoordinated His/− hemes are shown in black. (*e*) Cryo–electron microscopy structure of OmcS nanowire from *Geobacter sulfurreducens* (PDB ID: 6EF8) shown as a transparent surface with each OmcS monomer shown in a different color. The continuous heme chain through the nanowire is shown as sticks.

form a tight interaction with MtrAB and are likely to accept electrons through transient interactions. Surprisingly, early knockout studies showed that mutants lacking *mtrC* had a decrease in extracellular reduction, but it was necessary to also delete *omcA* to fully prevent EET to insoluble iron oxides. This indicated that OmcA can accept electrons from MtrAB in the absence of MtrC, despite being unable to form a stable complex (43). This suggests that the rate of EET is limited by intracellular metabolism, rather than the flux of electrons through MtrCAB. OmcA and UndA on the cell surface are likely to adopt a range of different conformations, as they are most likely tethered by a diacyl lipid anchor and there is no evidence to suggest interaction of the cytochrome with the lipid moiety (57). One potential role for OmcA or UndA could be to increase the number of OMCs on the cell surface in order to increase the range of potential substrates, increase the capacitance of the cell, and allow reduction of substrates that are not fully accessible by MtrC.

The arrangement of the heme domains in the *Shewanella* OMC is unusual, as the structures of other multiheme cytochromes have hemes packed either into a single domain or within adjacent domains that allow for rapid and continuous electron transfer (58). In the OMC, the two multiheme domains are separated by a β-barrel domain. The multiheme domains must form a stable noncovalent interaction to allow electron exchange between the two domains. The two halves of the OMC are connected by an α-helix containing a kink that increases flexibility, as revealed by the crystal structure of soluble MtrC in *S. baltica* OS185 and solution X-ray studies of MtrC from *S. oneidensis* (39, 59). Disruption of this helix would allow for rotation of the two OMC halves and break the electron transport chain through the OMC. Only 2–3 hydrogen bonds stabilize the OMC interface (**Figure 3*b***); furthermore, MtrC has been shown to contain a fully conserved disulfide bond that controls flavin reduction in the presence or absence of oxygen (55). It seems likely that formation of the disulfide bond under oxic conditions somehow triggers the separation of the two multiheme domains, breaking the electron transfer chain of MtrC. This would explain the unusual domain arrangement of the OMCs, but it is not yet clear how disulfide bond formation would trigger such an event.

Cell-Surface Cytochromes from Gram-Positive Bacteria

As Gram-positive bacteria do not have an outer membrane, they lack OMCs or porin–cytochrome complexes. Nevertheless, Gram-positive bacteria are still capable of EET through a range of different mechanisms (60). Both *Thermincola ferriacetica* and *Carboxydothermus ferrireducens* have been shown to reduce metal oxides through EET (61, 62). These bacteria are covered in CSCs that are associated with the proteinaceous S-layer that surrounds the cell and are proposed to receive electrons from the intermembrane space through an electron transfer network that permeates the S-layer. While the mechanism of electron transfer through the *C. ferrireducens* cell wall is not yet known, for *T. ferriacetica*, a *c*-type cytochrome is proposed to form a continuous heme chain across the membrane, allowing rapid electron transfer to the surface of the S-layer (63).

The structures of the CSC proteins OmhA and OcwA from *C. ferrireducens* and *T. ferriacetica* have both been resolved using X-ray crystallography (64, 65). OcwA and OmhA are CSCs containing 9 and 11 *c*-type hemes, respectively, that share little sequence identity but have substantial structural homology in terms of the packing of the hemes within the overall protein structure (**Figure 3*c*,*d***).

Within each CSC, nine of the hemes can be superimposed and share a similar arrangement with the highly conserved NrfA and HAO heme-packing motif (63). Of the nine shared hemes in OmhA and OcwA, seven are bis-His hexacoordinated, one is His–Met hexacoordinated and one is pentacoordinated. The extra two hemes of OmhA are both hexacoordinated, one is bis-His coordinated, while the other is coordinated by the N-terminal amine of the first amino acid in the peptide chain. While unusual, this novel packing is not completely uncommon and has been observed in other cytochromes such as the CooA sensor protein, in which the N-terminal proline forms the axial ligand to a heme and can be displaced in the presence of CO (66).

While there is no clear separation of domains like in the *Shewanella* OMCs, the assembly of the CSCs suggests clear flexibility in comparison to other members of the NrfA/HAO family; this could increase exposure of heme groups to the extracellular environment or introduce conformational flexibility in order to adjust the flow of electrons through the cytochrome.

The orientation of OcwA on the S-layer surface is not known. However, the OmhA monomer contains a domain that has significant homology to S-layer proteins and is proposed to form an integral connection with other proteins within the S-layer. This provides an orientation of OmhA such that the N-terminal heme 1 is the most likely site of electron ingress; hemes 9 or 11 would be positioned furthest away from the cell surface and consequently are most likely to reduce insoluble substrates. The high-spin heme would be exposed on one side of the structure and accessible to soluble substrates from the environment. The arrangement of pentacoordinated and His–Met-coordinated hemes is conserved within both structures, and in OcwA, these hemes have been shown to be capable of catalyzing the reduction of multiple soluble substrates such as nitrite or hydroxylamine in addition to insoluble ferrihydrite. OcwA has therefore been suggested to function like a Swiss Army knife and reduce a broad variety of soluble and insoluble substrates (65), providing extracellular respiratory flexibility. If so, it is similar to the OMCs of *Shewanella*, which have also been shown to reduce a range of both organic and inorganic substrates.

Geobacter Nanowires and Cables

The final group of extracellular cytochromes that have been structurally characterized are the polymeric cytochrome nanowires that are secreted by anaerobic bacteria such as *Geobacter*. These nanowires are predicted to be ubiquitous in nature and have been identified in both bacteria and archaea (67, 68). To date, four polymeric nanowires have been structurally characterized, including OmcS, OmcE, and OmcZ from *G. sulfurreducens*. OmcS was the first wire to be structurally resolved in 2019, through the use of cryo-EM (**Figure 3*e***) (69). This cytochrome was first identified as being important for Fe(III) oxide reduction; later, the use of immunogold labeling showed that OmcS was present in the conductive fibers that were produced by *G. sulfurreducens* (70), but it was not clear how the structure of OmcS could be involved in mineral reduction. Cryo-EM revealed that the OmcS polymer was composed of ∼5-nm long subunits that contained six *c*-type hemes. These OmcS are largely buried in the protein structure except at the termini of the chain where electrons are likely to enter and exit. Subsequently the tetraheme OmcE polymeric nanowire was also characterized from filaments sheared from *G. sulfurreducens* cells. OmcS and OmcE have significantly different protein structures but have a highly homologous arrangement of hemes within the structures, suggesting an optimized electron transfer pathway through the nanowire. Key to

this optimal electron transfer pathway is that the terminal hemes of each subunit are coordinated by a histidine in the adjacent subunit. The final polymeric nanowire to be recently characterized by cryo-EM is OmcZ, which has eight *c*-type hemes in a different configuration to that of the OmcS and OmcE hemes (71). The OmcZ heme arrangement causes branching of the heme chain resulting in three potential electron ingress/egress sites. There is no heme coordination between OmcZ subunits, which increases the distance between the hemes of adjacent subunits and may decrease the rate of electron transfer. Surprisingly these OmcZ nanowires are more conductive than OmcS nanowires, which may be due to the hemes of OmcZ being more accessible (72).

These polymeric nanowires are not necessarily involved in electron transfer across the outer membrane. *G. sulfurreducens* also contains at least five different porin–cytochrome complexes that have been shown to be essential for extracellular reduction of different substrates (25). Deletion of these complexes removes the ability of *G. sulfurreducens* to reduce extracellular metals, suggesting that the polymeric nanowires OmcS, OmcZ, and OmcE must obtain electrons through these porin–cytochrome complexes. The interactions between the nanowires and outer-membrane complexes are not yet known.

ASSEMBLY OF EXTRACELLULAR ELECTRON TRANSPORT SYSTEMS

The correct localization of any electron transport protein is critical to its function, and this is particularly so for an EET system that must be localized to the cell surface or extracellular milieu. There is still much to be learned about the assembly of model EET systems, and given the diversity of electron transport systems now emerging, there will also be a diversity of assembly processes to resolve. Understanding the biosynthesis and assembly of such systems will be important for future efforts to engineer new strains optimized for biotechnological applications through either homologous or heterologous expression. As an illustration of the challenges of assembling an EET system interfaced to intracellular metabolism, we focus on the *Shewanella* spp. porin–cytochrome complexes and OMCs.

The localization and assembly of an OMC requires that the polypeptide be exported first across the inner membrane to the periplasm and then across the outer membrane. The assembly of periplasmic *c*-type cytochromes has been widely studied in a phylogenetically wide range of bacteria. In general terms, the translated polypeptide is exported across the cytoplasmic membrane via the Sec system, and hemes are covalently attached through the action of heme-lyase components of various cytochrome *c* maturation (Ccm) systems. There are some variants of such systems in different species, including systems dedicated to the attachment of hemes to nonstandard heme-binding motifs (e.g., CXXCK rather than CXXCH) (73, 74). *S. oneidensis* has multiple copies of genes encoding Ccm systems, suggesting some functional overlap, but the capacity for Fe(III) or Mn(IV) respiration is compromised in various deletion mutants in these systems, consistent with a role in holo-OMC protein maturation (74). It is likely that hemes are attached to the polypeptide chain as it emerges from the Sec system and that protein folding around hemes occurs in the periplasm. Thereafter, the folded multiheme protein must be exported to the extracellular face of the protein. Genetic evidence suggests that this is manifested though a type II secretion system (T2SS) (75, 76). This has been shown to be the case for OMCs expressed homologously in *S. oneidensis* (75) and heterologously in *Escherichia coli* (76). In both cases, the OMC proteins could be detected in the T2SS mutants but were mislocated to the periplasm, as judged by the susceptibility of the OMCs to extracellular proteases (76). In *E. coli*, whole-cell visible spectroscopy confirmed that heterologously expressed holo-OMC had been correctly assembled in the T2SS mutant but was trapped in the periplasm and so unable to transfer electrons to an extracellular electron acceptor. It should be noted that some *E. coli* strains do not express functional T2SS, so the choice of host for heterologous expression is critical (75).

An additional complexity of the *Shewanella* OMCs is that they are lipoproteins, so acylation must also take place during the inner membrane–periplasmic stages of the biogenesis and assembly journey. The acylation is critical to localization at the outer face of the outer membrane since removal of the lipid-binding site results in release of the OMC into the extracellular environment. The process of lipoprotein acylation is generally understood in Gram-negative bacteria (77), with the attachment of the diacylglyceryl moiety to the N-terminal Cys-containing lipobox occurring while the protein is still attached by its signal peptide to the inner membrane (57). For *S. oneidensis*, lipo-OMC maturation is less well understood, as there must also be a message in the lipobox that ensures the released lipo-OMC avoids localization by the Lol system to the inner face of the outer membrane and can instead be directed to the T2SS for excretion to the outer face (78).

Having considered the assembly and localization of the extracellular OMCs, we now turn to the porin–cytochrome complexes and focus on *S. oneidensis* MtrAB, as this remains the only complex for which there is an experimentally determined structure. Two separate assembly processes must come together: the synthesis of an outer-membrane porin and the insertion of a mature holo-periplasmic multiheme cytochrome into the complex. *S. oneidensis* possesses the phylogenetically widespread β-barrel assembly machinery (79), but early studies found that MtrB was not detectable in *S. oneidensis* Δ*mtrA* mutants (38). An investigation into this phenomenon, including heterologous expression of *mtrAB* genes in *E. coli*, revealed that an interaction between MtrA and MtrB is required to prevent MtrB degradation (80). In both *S. oneidensis* and *E. coli*, this degradation is catalyzed by the protease DegP, which targets misfolded proteins. Thus, in addition to being a functional electron transport component of the porin–cytochrome complex, MtrA appears to function as a periplasmic chaperone for MtrB prior to correct insertion into the outer membrane. The molecular nature of the MtrAB interaction as the complex matures in the periplasm is not yet known.

HOMOLOGY MODELING OF PORIN–CYTOCHROME COMPLEXES

The recent advent of artificial intelligence–assisted modeling of proteins based on their amino acid sequences through programs such as AlphaFold has revolutionized the understanding of previously uncharacterized proteins, allowing for structural predictions of proteins with little homology to experimentally determined structures (81). For example, an early AlphaFold-based structural and mechanistic model was proposed for Cyc2 with two Fe-binding sites, generated by Tyr262/Asp308 and His119/Asp137/Asp138, within the central cavity of the porin, forming a separate heme domain at the base of the cytochrome (82). The recent development of AlphaFold 3 allowed the generation of a new Cyc2 structural model that includes a *c*-type heme more realistically embedded within the base of the structure and coordinated by a histidine and N-terminal proline or leucine. The originally proposed Fe-binding sites are substantially shifted: Tyr262 and Asp308 are no longer close enough to form an Fe-binding site, while His119, Asp137, and Asp138 are now close enough to generate an Fe-binding site with the addition of the heme propionate group (**Figure 4*a***). The Cyc2 model interior is strongly electronegative, which would have significant impact on the binding and release of positively charged Fe^{3+} ions (**Figure 4*b***). The highly negative interior is also present in AlphaFold models of the three Cyc2 proteins from both *S. lithotrophicus* ES-1 and Cyc2PV-1 from *M. ferrooxydans*, suggesting it is also important under neutrophilic conditions (49, 50). These five structural models also have an N-terminal proline, leucine, or valine close to the proximal side of the heme Fe and could likely coordinate the heme iron. N-terminal proline coordination is observed in cytochromes such as CooA (83), in which the N-terminal ligand can be exchanged for CO. It is not clear why an N-terminal amine would be part of the Cyc2 heme coordination, but the redox potentials measured for CooA isolated from

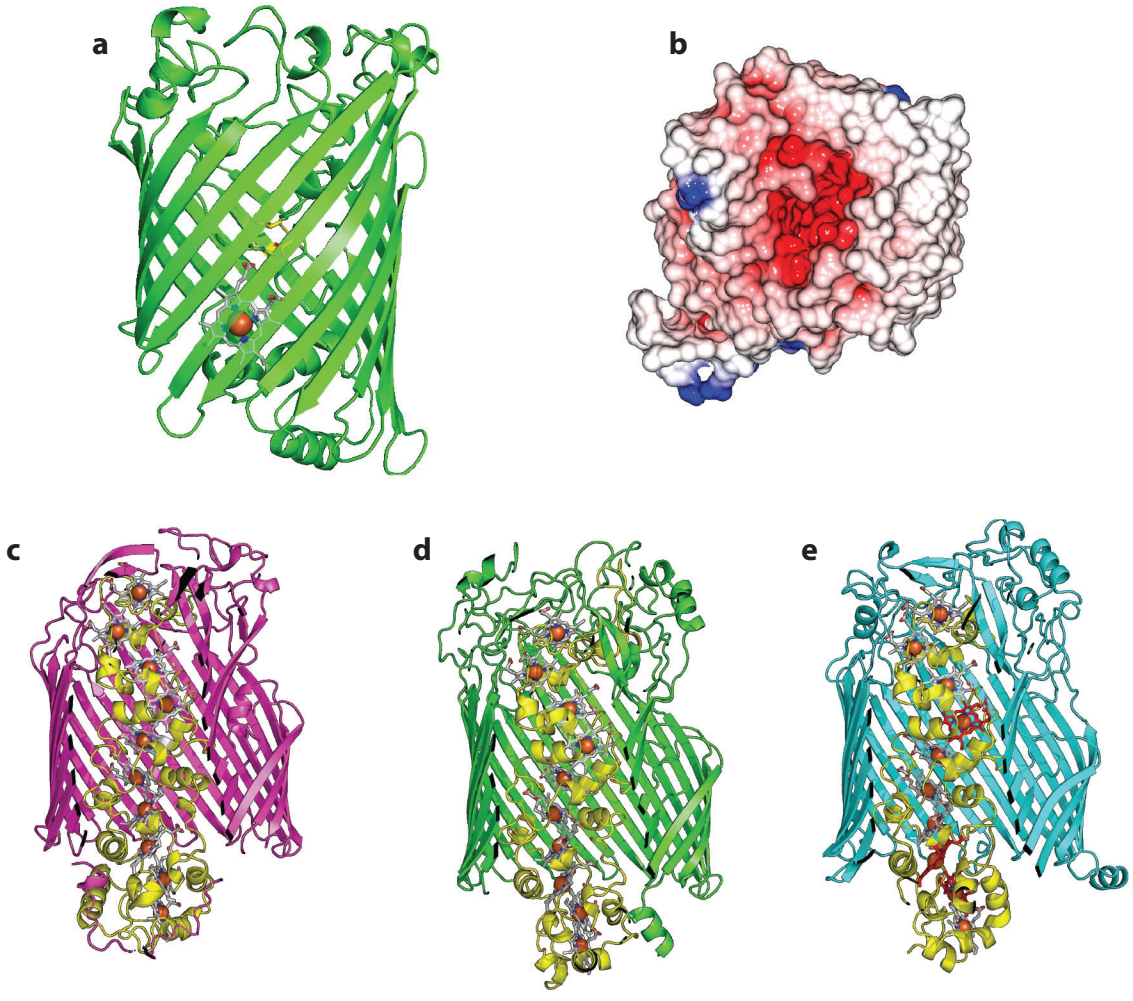

Figure 4

AlphaFold 3 models of porin–cytochromes known to be involved in extracellular electron transfer. (*a*) Cyc2 from *Acidithiobacillus ferrooxidans*, shown in ribbon format with the periplasmic-facing heme shown as sticks. (*b*) Electrostatic potential surface map of Cyc2 generated using the *CCP4mg* molecular-graphics software and oriented to show the extracellular-facing side of the porin. (*c*) MtrDE from *Shewanella oneidensis*. (*d*) MtoAB from *Sideroxydans lithotrophicus* ES-1. (*e*) PioAB from *Rhodopseudomonas palustris* TIE-1. Complexes in panels *c*–*e* are shown in ribbon format, with porins colored magenta (MtrE), green (MtoB), and cyan (PioB). Embedded cytochromes are colored yellow, with porphyrin rings shown as white sticks and coordinating iron atoms as orange spheres.

Carboxydothermus hydrogenformans are approximately +230 mV compared to a standard hydrogen electrode, consistent with this heme being able to accept electrons from soluble Fe^{2+} (84).

AlphaFold 3 can also produce two-component porin–cytochrome complexes. These can provide further insight into the potential structure, likely topology, and EET mechanism. When the MtrDE, MtoAB, and PioAB porin–cytochrome complexes were modeled using AlphaFold (81, 85), models were generated with significant structural homology to MtrAB (**Figure 4*c*–*e***). All three models show the decaheme cytochrome subunit embedded within a porin subunit in an orientation that would allow electron transfer from one side of the membrane to another. MtrD and MtoA both have 10 bis-His-coordinated hemes, while the PioA model indicates hemes 2, 3, and

7 are His–Met coordinated. These are consistent with spectroscopic evidence provided from isolated MtoA and PioA showing evidence for bis-His and His–Met coordination, respectively (45, 48).

The cytochrome N termini are predicted to extend into the periplasm sufficiently for at least two hemes to be exposed for electron exchange with periplasmic redox partners. The C terminal of MtrD is exposed on the surface of the complex, most likely to form stable complexes with their redox partner, MtrF, on the surface of the cell (**Figure 4*c***). In contrast, both PioA and MtoA are largely buried within the complex, which is consistent with their roles in the selective oxidation of soluble Fe(II) (**Figure 4*d*,*e***). In this case, the extended loops may help in preventing the formation or accumulation of Fe(III) (hydr)oxide precipitates on the surface of the PioAB or MtoAB complex. Interestingly, transcriptomic data indicated that MtoAB was also involved with oxidation of the insoluble reduced iron smectite (27). It is not clear from this model how this would occur, but it could potentially involve another extracellular protein or siderophore on the *S. lithotrophicus* surface.

All three complexes also have significant channels to the side of the cytochrome within the porin. This was originally observed within the structure of MtrCAB and is generated by the excess β-strands that are not used in cytochrome binding. These channels could be involved in the passive diffusion of water through the structure or potentially in the transport of protons. The similarity between the four MtrAB orthologs is sufficient to produce models with relative confidence that reveal the conservation of the side channel.

The five porin–cytochrome complexes of *G. sulfurreducens* are essential for electron transfer across the outer membrane but have little homology to any experimentally determined complexes. These five complexes include OmaB–OmbB–OmcB (Gpc1), OmaC–OmbC–OmcC (Gpc2), ExtABCD, ExtEFG, and ExtHIJK. Gpc1 and Gpc2 appear to have arisen due to a gene duplication and have been retained in all *Geobacter* species, suggesting a strong dependence on these complexes. They were also shown to play an important role in reduction of Fe(III) citrate and ferrihydrite (37, 86). *G. sulfurreducens* current production was shown to be heavily dependent on expression of *extABCD* (25, 87). While ExtABCD is important for growth on electrodes it is not essential for Fe(III) oxide reduction (88). Expression of *extEFG* is upregulated in *G. sulfurreducens* grown on electrodes at high potentials (89), with research suggesting that ExtEFG is not important for reduction of Fe(III) oxides but plays at least a partial role in the reduction of Mn(IV) oxides (25). A strong phenotype for the ExtHIJKL complex has yet to been shown; however, researchers have demonstrated the importance of ExtI, the porin component of the complex, as a transporter of selenite into the cell (90). This suggests the possibility that ExtHIJKL does not play a role in extracellular electron transport and instead acts as a selenite uptake and detoxifier system (91).

AlphaFold 3 models of the *G. sulfurreducens* porin–cytochrome complexes are substantially different to the previously characterized complexes (**Figure 5**). Gpc1 and Gpc2 are very similar, with the 8-heme cytochrome positioned within the β-barrel and capped by 12-heme surface cytochromes (**Figure 5*a***). ExtEFG and ExtBCD have similar five-heme transmembrane cytochromes but very different surface cytochromes. AlphaFold 3 modeling of ExtI generated a β-barrel with a C-terminal domain plugging the barrel. This is consistent with a potential role for ExtHIJKL in selenite detoxification but not in the formation of a porin–cytochrome complex capable of transmembrane electron transfer.

Overall, the *G. sulfurreducens* transmembrane porin–cytochromes are smaller and lack the longer loops that help to stabilize the interactions between periplasmic cytochrome and porin on the surface of the cell. The porin solvent channel is present in ExtBC but not in the other predicted complexes (**Figure 5*b***). The shortness of the barrels means that only five hemes are required to transfer electrons across the membrane, with both ExtC and ExtF being contained

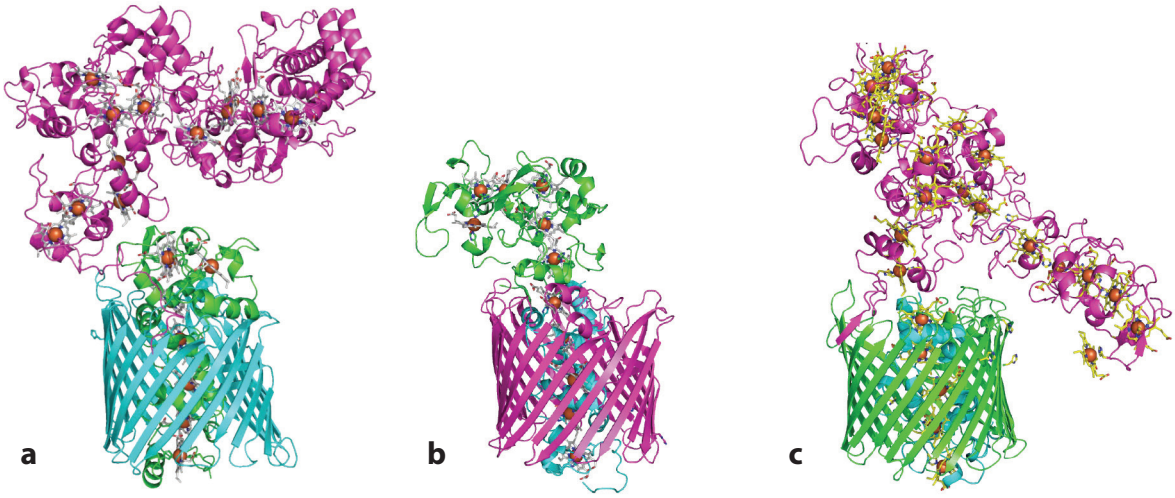

Figure 5

AlphaFold 3 models of porin–cytochrome complexes from *Geobacter sulfurreducens*. Models are shown in ribbon form with porphyrin rings shown as yellow sticks and iron atoms as orange spheres. (*a*) Gpc1 complex consisting of octaheme OmaB (*green*), porin OmbB (*cyan*), and dodecaheme OmcB (*magenta*). (*b*) ExtBCD complex consisting of pentaheme ExtC (*cyan*), porin ExtB (*magenta*), and hexaheme ExtD (*green*). (*c*) ExtEFG complex consisting of pentaheme ExtF (*cyan*), porin ExtE (*green*), and icosaheme ExtG (*magenta*).

within ExtB and ExtE respectively. Previously, both ExtC and ExtF were predicted to be extracellular due to the presence of a C-terminal lipid anchor, so the positioning of these pentaheme cytochromes is unexpected. The remaining three hemes of the octaheme OmaB and OmcB lie across the outer surface of the barrel, available for electron transfer. The models of the 12-heme CSCs for OmcB and OmcC are highly similar and contain 12 bis-His-coordinated *c*-type hemes. Both structures have a highly exposed heme 1 that serves as the ingress site for electrons from the corresponding porin–cytochrome complex. The height of the Gpc1 and Gpc2 complexes from the hydrophobic core of the outer membrane could reach ~90–100 Å, similar to the MtrCAB complex, but the predicted structures suggest that the heme chains are capped by an ~150–amino acid cap that would restrict direct electron transfer to extracellular insoluble substrates. This is surprising, as it limits the number of potential substrates that can be transferred and suggests that these proteins have a specific role in regulating EET.

In contrast to OmcB and OmcA, the AlphaFold model of the hexaheme ExtD suggests a remarkably truncated structure that reaches a maximum of only ~40 Å above the membrane surface (**Figure 5*b***). While it is unclear how this shortened surface cytochrome would react with electrodes, the distance between the adjacent hemes of ExtC and ExtD is <6 Å, indicating that electron transfer could be very fast, which could explain how ExtBCD increases current production by *G. sulfurreducens*.

Like the other *G. sulfurreducens* porin–cytochrome complexes the ExtEFG complex is predicted to consist of a pentaheme cytochrome (ExtF) encased within a porin and capped by a surface cytochrome (ExtG) (**Figure 5*c***). The interheme distance between ExtF and ExtG cytochrome is ~7.5 Å, suggesting rapid electron transfer, while ExtG is predicted to be an extracellular 20-heme chain. The terminal heme is poorly modeled and exposed, suggesting there is something unusual about this heme and that either the packing within the structure cannot currently be predicted or it is an interdomain heme that requires coordination by an adjacent protein, similar to the terminal heme of OmcS.

CONCLUDING REMARKS: THE FUTURE OF EXTRACELLULAR ELECTRON TRANSFER STUDY

After EET was identified as a common metabolic feature of many bacteria, it was not clear whether the systems responsible for extracellular reduction were conserved or convergent evolution was responsible for the formation of a disparate range of transporters across different bacterial classes. Identification of the MtrCAB porin–cytochrome cluster in *Shewanella* made it possible to identify similar gene clusters across different bacterial classes that conferred EET to the host organism, such as *R. palustris* TIE-1 and *S. lithotrophicus*, but these gene clusters were missing in other model bacteria, such as *Geobacter*. Subsequently, careful analysis of the genome of *G. sulfurreducens* revealed the genes for novel porin–cytochrome complexes that had no homology to the canonical *mtr* gene clusters. The challenges associated with purification and characterization of these new clusters mean little biochemical information is currently available, but modern protein modeling software provides clues that can help drive the development of new hypotheses for why organisms often require a range of different EET mechanisms. EET is likely a mixture of conserved and convergent evolution: The transfer of EET gene clusters provides a competitive advantage, but there are many potential mechanisms for EET in different environments, and it is likely that, through evolution, different systems have appeared repeatedly. The myriad of different mechanisms for EET that are likely undiscovered within the genomes of bacteria and other organisms will provide opportunities for research for many years to come.

DISCLOSURE STATEMENT

The authors are not aware of any affiliations, memberships, funding, or financial holdings that might be perceived as affecting the objectivity of this review.

ACKNOWLEDGMENTS

This research was supported by the United Kingdom Research and Innovation Biotechnology and Biological Sciences Research Council (BB/X011453/1 and BB/P01819X/1 to T.A.C. and D.J.R.) and a University of East Anglia studentship awarded to J.A.J.B. The authors are grateful to Julea Butt, Benjamin Nash, and Alejandro Morales-Florez for useful discussions.

LITERATURE CITED

1. White GF, Edwards MJ, Gomez-Perez L, Richardson DJ, Butt JN, Clarke TA. 2016. Mechanisms of bacterial extracellular electron exchange. *Adv. Microb. Physiol.* 68:87–138
2. Lovley DR. 2012. Electromicrobiology. *Annu. Rev. Microbiol.* 66:391–409
3. Shi L, Dong H, Reguera G, Beyenal H, Lu A, et al. 2016. Extracellular electron transfer mechanisms between microorganisms and minerals. *Nat. Rev. Microbiol.* 14:651–62
4. Lusk BG. 2019. Thermophiles; or, the modern Prometheus: the importance of extreme microorganisms for understanding and applying extracellular electron transfer. *Front. Microbiol.* 10:818
5. Nealson KH, Belz A, McKee B. 2002. Breathing metals as a way of life: geobiology in action. *Antonie Van Leeuwenhoek* 81:215–22
6. Roberto FF, Schippers A. 2022. Progress in bioleaching: part B, applications of microbial processes by the minerals industries. *Appl. Microbiol. Biotechnol.* 106:5913–28
7. Gujjala LKS, Dutta D, Sharma P, Kundu D, Vo DN, Kumar S. 2022. A state-of-the-art review on microbial desalination cells. *Chemosphere* 288:132386
8. Beblawy S, Philipp LA, Gescher J. 2020. Accelerated electro-fermentation of acetoin in *Escherichia coli* by identifying physiological limitations of the electron transfer kinetics and the central metabolism. *Microorganisms* 8:1843

9. Roy R, Samanta S, Pandit S, Naaz T, Banerjee S, et al. 2024. An overview of bacteria-mediated heavy metal bioremediation strategies. *Appl. Biochem. Biotechnol.* 196:1712–51
10. Mishra S, Ghosh S, van Hullebusch ED, Singh S, Das AP. 2023. A critical review on the recovery of base and critical elements from electronic waste-contaminated streams using microbial biotechnology. *Appl. Biochem. Biotechnol.* 195:7859–88
11. Light SH, Su L, Rivera-Lugo R, Cornejo JA, Louie A, et al. 2018. A flavin-based extracellular electron transfer mechanism in diverse Gram-positive bacteria. *Nature* 562:140–44
12. Hederstedt L, Gorton L, Pankratova G. 2020. Two routes for extracellular electron transfer in *Enterococcus faecalis*. *J. Bacteriol.* 202:e00725-19
13. Saunders SH, Tse ECM, Yates MD, Otero FJ, Trammell SA, et al. 2020. Extracellular DNA promotes efficient extracellular electron transfer by pyocyanin in *Pseudomonas aeruginosa* biofilms. *Cell* 182:919–32.e19
14. Howley E, Mangus A, Williams D, Torres CI. 2023. Intracytoplasmic membranes develop in *Geobacter sulfurreducens* under thermodynamically limiting conditions. *npj Biofilms Microbiomes* 9:18
15. Richardson DJ, Butt JN, Clarke TA. 2013. Controlling electron transfer at the microbe–mineral interface. *PNAS* 110:7537–38
16. Rivera-Lugo R, Huang S, Lee F, Meheust R, Iavarone AT, et al. 2023. Distinct energy-coupling factor transporter subunits enable flavin acquisition and extracytosolic trafficking for extracellular electron transfer in *Listeria monocytogenes*. *mBio* 14:e0308522
17. Carlson HK, Iavarone AT, Gorur A, Yeo BS, Tran R, et al. 2012. Surface multiheme *c*-type cytochromes from *Thermincola potens* and implications for respiratory metal reduction by Gram-positive bacteria. *PNAS* 109:1702–7
18. Bird LJ, Bonnefoy V, Newman DK. 2011. Bioenergetic challenges of microbial iron metabolisms. *Trends Microbiol.* 19:330–40
19. Myers CR, Nealson KH. 1988. Bacterial manganese reduction and growth with manganese oxide as the sole electron acceptor. *Science* 240:1319–21
20. Lovley DR, Phillips EJ. 1988. Novel mode of microbial energy metabolism: organic carbon oxidation coupled to dissimilatory reduction of iron or manganese. *Appl. Environ. Microbiol.* 54:1472–80
21. Emerson D, Floyd MM. 2005. Enrichment and isolation of iron-oxidizing bacteria at neutral pH. *Methods Enzymol.* 397:112–23
22. Ingledew WJ. 1982. *Thiobacillus ferrooxidans*. The bioenergetics of an acidophilic chemolithotroph. *Biochim. Biophys. Acta Rev. Bioenerg.* 683:89–117
23. Beliaev AS, Saffarini DA. 1998. *Shewanella putrefaciens mtrB* encodes an outer membrane protein required for Fe(III) and Mn(IV) reduction. *J. Bacteriol.* 180:6292–97
24. Yarzabal A, Brasseur G, Ratouchniak J, Lund K, Lemesle-Meunier D, et al. 2002. The high-molecular-weight cytochrome *c* Cyc2 of *Acidithiobacillus ferrooxidans* is an outer membrane protein. *J. Bacteriol.* 184:313–17
25. Jimenez Otero F, Chan CH, Bond DR. 2018. Identification of different putative outer membrane electron conduits necessary for Fe(III) citrate, Fe(III) oxide, Mn(IV) oxide, or electrode reduction by *Geobacter sulfurreducens*. *J. Bacteriol.* 200:e00347-18
26. He S, Barco RA, Emerson D, Roden EE. 2017. Comparative genomic analysis of neutrophilic iron(II) oxidizer genomes for candidate genes in extracellular electron transfer. *Front. Microbiol.* 8:1584
27. Zhou N, Kupper RJ, Catalano JG, Thompson A, Chan CS. 2022. Biological oxidation of Fe(II)-bearing smectite by microaerophilic iron oxidizer *Sideroxydans lithotrophicus* using dual Mto and Cyc2 iron oxidation pathways. *Environ. Sci. Technol.* 56:17443–53
28. Glasser NR, Kern SE, Newman DK. 2014. Phenazine redox cycling enhances anaerobic survival in *Pseudomonas aeruginosa* by facilitating generation of ATP and a proton-motive force. *Mol. Microbiol.* 92:399–412
29. Feng J, Jiang M, Li K, Lu Q, Xu S, et al. 2020. Direct electron uptake from a cathode using the inward Mtr pathway in *Escherichia coli*. *Bioelectrochemistry* 134:107498
30. Jensen HM, Albers AE, Malley KR, Londer YY, Cohen BE, et al. 2010. Engineering of a synthetic electron conduit in living cells. *PNAS* 107:19213–18

31. Mouhib M, Reggente M, Li L, Schuergers N, Boghossian AA. 2023. Extracellular electron transfer pathways to enhance the electroactivity of modified *Escherichia coli*. *Joule* 7:2092–106
32. Appia-Ayme C, Guiliani N, Ratouchniak J, Bonnefoy V. 1999. Characterization of an operon encoding two *c*-type cytochromes, an aa_3-type cytochrome oxidase, and rusticyanin in *Thiobacillus ferrooxidans* ATCC 33020. *Appl. Environ. Microbiol.* 65:4781–87
33. White GF, Shi Z, Shi L, Wang Z, Dohnalkova AC, et al. 2013. Rapid electron exchange between surface-exposed bacterial cytochromes and Fe(III) minerals. *PNAS* 110:6346–51
34. Stikane A, Hwang ET, Ainsworth EV, Piper SEH, Critchley K, et al. 2019. Towards compartmentalized photocatalysis: multihaem proteins as transmembrane molecular electron conduits. *Faraday Discuss.* 215:26–38
35. Edwards MJ, White GF, Lockwood CW, Lawes MC, Martel A, et al. 2018. Structural modeling of an outer membrane electron conduit from a metal-reducing bacterium suggests electron transfer via periplasmic redox partners. *J. Biol. Chem.* 293:8103–12
36. Piper SEH, Casadevall C, Reisner E, Clarke TA, Jeuken LJC, et al. 2022. Photocatalytic removal of the greenhouse gas nitrous oxide by liposomal microreactors. *Angew. Chem. Int. Ed.* 61:e202210572
37. Liu Y, Wang Z, Liu J, Levar C, Edwards MJ, et al. 2014. A trans-outer membrane porin-cytochrome protein complex for extracellular electron transfer by *Geobacter sulfurreducens* PCA. *Environ. Microbiol. Rep.* 6:776–85
38. Hartshorne RS, Reardon CL, Ross D, Nuester J, Clarke TA, et al. 2009. Characterization of an electron conduit between bacteria and the extracellular environment. *PNAS* 106:22169–74
39. Edwards MJ, White GF, Butt JN, Richardson DJ, Clarke TA. 2020. The crystal structure of a biological insulated transmembrane molecular wire. *Cell* 181:665–73.e10
40. Lockwood CWJ, van Wonderen JH, Edwards MJ, Piper SEH, White GF, et al. 2018. Membrane-spanning electron transfer proteins from electrogenic bacteria: production and investigation. *Methods Enzymol.* 613:257–75
41. Jiang X, van Wonderen JH, Butt JN, Edwards MJ, Clarke TA, Blumberger J. 2020. Which multi-heme protein complex transfers electrons more efficiently? Comparing MtrCAB from *Shewanella* with OmcS from *Geobacter*. *J. Phys. Chem. Lett.* 11:9421–25
42. Clarke TA. 2022. Plugging into bacterial nanowires: a comparison of model electrogenic organisms. *Curr. Opin. Microbiol.* 66:56–62
43. Coursolle D, Gralnick JA. 2010. Modularity of the Mtr respiratory pathway of *Shewanella oneidensis* strain MR-1. *Mol. Microbiol.* 77:995–1008
44. Bucking C, Piepenbrock A, Kappler A, Gescher J. 2012. Outer-membrane cytochrome-independent reduction of extracellular electron acceptors in *Shewanella oneidensis*. *Microbiology* 158:2144–57
45. Liu J, Wang Z, Belchik SM, Edwards MJ, Liu C, et al. 2012. Identification and characterization of MtoA: a decaheme *c*-type cytochrome of the neutrophilic Fe(II)-oxidizing bacterium *Sideroxydans lithotrophicus* ES-1. *Front. Microbiol.* 3:37
46. Beckwith CR, Edwards MJ, Lawes M, Shi L, Butt JN, et al. 2015. Characterization of MtoD from *Sideroxydans lithotrophicus*: a cytochrome c electron shuttle used in lithoautotrophic growth. *Front. Microbiol.* 6:332
47. Gupta D, Sutherland MC, Rengasamy K, Meacham JM, Kranz RG, Bose A. 2019. Photoferrotrophs produce a PioAB electron conduit for extracellular electron uptake. *mBio* 10:e02668-19
48. Li DB, Edwards MJ, Blake AW, Newton-Payne SE, Piper SEH, et al. 2020. His/Met heme ligation in the PioA outer membrane cytochrome enabling light-driven extracellular electron transfer by *Rhodopseudomonas palustris* TIE-1. *Nanotechnology* 31:354002
49. Zhou N, Keffer JL, Polson SW, Chan CS. 2022. Unraveling Fe(II)-oxidizing mechanisms in a facultative Fe(II) oxidizer, *Sideroxydans lithotrophicus* strain ES-1, via culturing, transcriptomics, and reverse transcription-quantitative PCR. *Appl. Environ. Microbiol.* 88:e0159521
50. McAllister SM, Polson SW, Butterfield DA, Glazer BT, Sylvan JB, Chan CS. 2020. Validating the Cyc2 neutrophilic iron oxidation pathway using meta-omics of *Zetaproteobacteria* iron mats at marine hydrothermal vents. *mSystems* 5:e00553-19
51. Keffer JL, McAllister SM, Garber AI, Hallahan BJ, Sutherland MC, et al. 2021. Iron oxidation by a fused cytochrome-porin common to diverse iron-oxidizing bacteria. *mBio* 12:e0107421

52. Clarke TA, Edwards MJ, Gates AJ, Hall A, White GF, et al. 2011. Structure of a bacterial cell surface decaheme electron conduit. *PNAS* 108:9384–89
53. Edwards MJ, Hall A, Shi L, Fredrickson JK, Zachara JM, et al. 2012. The crystal structure of the extracellular 11-heme cytochrome UndA reveals a conserved 10-heme motif and defined binding site for soluble iron chelates. *Structure* 20:1275–84
54. Edwards MJ, Baiden NA, Johs A, Tomanicek SJ, Liang L, et al. 2014. The X-ray crystal structure of *Shewanella oneidensis* OmcA reveals new insight at the microbe–mineral interface. *FEBS Lett*. 588:1886–90
55. Edwards MJ, White GF, Norman M, Tome-Fernandez A, Ainsworth E, et al. 2015. Redox linked flavin sites in extracellular decaheme proteins involved in microbe-mineral electron transfer. *Sci. Rep.* 5:11677
56. Edwards MJ, Gates AJ, Butt J, Richardson DJ, Clarke TA. 2017. Comparative structure-potentio-spectroscopy of the *Shewanella* outer membrane multiheme cytochromes. *Curr. Opin. Electrochem.* 4:199–205
57. van Wonderen JH, Crack JC, Edwards MJ, Clarke TA, Saalbach G, et al. 2024. Liquid-chromatography mass spectrometry describes post-translational modification of *Shewanella* outer membrane proteins. *Biochim. Biophys. Acta Biomembr.* 1866:184221
58. Edwards MJ, Richardson DJ, Paquete CM, Clarke TA. 2020. Role of multiheme cytochromes involved in extracellular anaerobic respiration in bacteria. *Protein Sci*. 29:830–42
59. Norman MP, Edwards MJ, White GF, Burton JAJ, Butt JN, et al. 2023. A cysteine pair controls flavin reduction by extracellular cytochromes during anoxic/oxic environmental transitions. *mBio* 14:e0258922
60. Gomaa OM, Costa NL, Paquete CM. 2022. Electron transfer in Gram-positive bacteria: enhancement strategies for bioelectrochemical applications. *World J. Microbiol. Biotechnol.* 38:83
61. Parameswaran P, Bry T, Popat SC, Lusk BG, Rittmann BE, Torres CI. 2013. Kinetic, electrochemical, and microscopic characterization of the thermophilic, anode-respiring bacterium *Thermincola ferriacetica*. *Environ. Sci. Technol.* 47:4934–40
62. Gavrilov SN, Lloyd JR, Kostrikina NA, Slobodkin AI. 2012. Fe(III) oxide reduction by a Gram-positive thermophile: physiological mechanisms for dissimilatory reduction of poorly crystalline Fe(III) oxide by a thermophilic Gram-positive bacterium *Carboxydothermus ferrireducens*. *Geomicrobiol. J.* 29:804–19
63. Faustino MM, Fonseca BM, Costa NL, Lousa D, Louro RO, Paquete CM. 2021. Crossing the wall: characterization of the multiheme cytochromes involved in the extracellular electron transfer pathway of *Thermincola ferriacetica*. *Microorganisms* 9:293
64. Tikhonova TV, Osipov EM, Dergousova NI, Boyko KM, Elizarov IM, et al. 2023. Extracellular Fe(III) reductase structure reveals a modular organization enabling S-layer insertion and electron transfer to insoluble substrates. *Structure* 31:174–84.e3
65. Costa NL, Hermann B, Fourmond V, Faustino MM, Teixeira M, et al. 2019. How thermophilic Gram-positive organisms perform extracellular electron transfer: characterization of the cell surface terminal reductase OcwA. *mBio* 10:e01210-19
66. Borjigin M, Li H, Lanz ND, Kerby RL, Roberts GP, Poulos TL. 2007. Structure-based hypothesis on the activation of the CO-sensing transcription factor CooA. *Acta Crystallogr. D Biol. Crystallogr.* 63:282–87
67. Wang F, Mustafa K, Suciu V, Joshi K, Chan CH, et al. 2022. Cryo-EM structure of an extracellular *Geobacter* OmcE cytochrome filament reveals tetrahaem packing. *Nat. Microbiol.* 7:1291–300
68. Baquero DP, Cvirkaite-Krupovic V, Hu SS, Fields JL, Liu X, et al. 2023. Extracellular cytochrome nanowires appear to be ubiquitous in prokaryotes. *Cell* 186:2853–64.e8
69. Wang F, Gu Y, O'Brien JP, Yi SM, Yalcin SE, et al. 2019. Structure of microbial nanowires reveals stacked hemes that transport electrons over micrometers. *Cell* 177:361–69.e10
70. Leang C, Qian X, Mester T, Lovley DR. 2010. Alignment of the *c*-type cytochrome OmcS along pili of *Geobacter sulfurreducens*. *Appl. Environ. Microbiol.* 76:4080–84
71. Gu Y, Guberman-Pfeffer MJ, Srikanth V, Shen C, Giska F, et al. 2023. Structure of *Geobacter* cytochrome OmcZ identifies mechanism of nanowire assembly and conductivity. *Nat. Microbiol.* 8:284–98
72. Yalcin SE, O'Brien JP, Gu Y, Reiss K, Yi SM, et al. 2020. Electric field stimulates production of highly conductive microbial OmcZ nanowires. *Nat. Chem. Biol.* 16:1136–42
73. Jin M, Jiang Y, Sun L, Yin J, Fu H, et al. 2013. Unique organizational and functional features of the cytochrome *c* maturation system in *Shewanella oneidensis*. *PLOS ONE* 8:e75610

74. Brockman KL, Shirodkar S, Croft TJ, Banerjee R, Saffarini DA. 2020. Regulation and maturation of the *Shewanella oneidensis* sulfite reductase SirA. *Sci. Rep.* 10:953
75. Shi L, Deng S, Marshall MJ, Wang Z, Kennedy DW, et al. 2008. Direct involvement of type II secretion system in extracellular translocation of *Shewanella oneidensis* outer membrane cytochromes MtrC and OmcA. *J. Bacteriol.* 190:5512–16
76. Donald JW, Hicks MG, Richardson DJ, Palmer T. 2008. The *c*-type cytochrome OmcA localizes to the outer membrane upon heterologous expression in *Escherichia coli*. *J. Bacteriol.* 190:5127–31
77. Nakayama H, Kurokawa K, Lee BL. 2012. Lipoproteins in bacteria: structures and biosynthetic pathways. *FEBS J.* 279:4247–68
78. Konovalova A, Silhavy TJ. 2015. Outer membrane lipoprotein biogenesis: Lol is not the end. *Philos. Trans. R. Soc. B* 370:20150030
79. Shen C, Chang S, Luo Q, Chan KC, Zhang Z, et al. 2023. Structural basis of BAM-mediated outer membrane β-barrel protein assembly. *Nature* 617:185–93
80. Schicklberger M, Bucking C, Schuetz B, Heide H, Gescher J. 2011. Involvement of the *Shewanella oneidensis* decaheme cytochrome MtrA in the periplasmic stability of the β-barrel protein MtrB. *Appl. Environ. Microbiol.* 77:1520–23
81. Jumper J, Evans R, Pritzel A, Green T, Figurnov M, et al. 2021. Highly accurate protein structure prediction with AlphaFold. *Nature* 596:583–89
82. Jiang V, Khare SD, Banta S. 2021. Computational structure prediction provides a plausible mechanism for electron transfer by the outer membrane protein Cyc2 from *Acidithiobacillus ferrooxidans*. *Protein Sci.* 30:1640–52
83. Lanzilotta WN, Schuller DJ, Thorsteinsson MV, Kerby RL, Roberts GP, Poulos TL. 2000. Structure of the CO sensing transcription activator CooA. *Nat. Struct. Biol.* 7:876–80
84. Inagaki S, Masuda C, Akaishi T, Nakajima H, Yoshioka S, et al. 2005. Spectroscopic and redox properties of a CooA homologue from *Carboxydothermus hydrogenoformans*. *J. Biol. Chem.* 280:3269–74
85. Abramson J, Adler J, Dunger J, Evans R, Green T, et al. 2024. Accurate structure prediction of biomolecular interactions with AlphaFold 3. *Nature* 630:493–500
86. Liu Y, Fredrickson JK, Zachara JM, Shi L. 2015. Direct involvement of *ombB*, *omaB*, and *omcB* genes in extracellular reduction of Fe(III) by *Geobacter sulfurreducens* PCA. *Front. Microbiol.* 6:1075
87. Jimenez Otero F, Chadwick GL, Yates MD, Mickol RL, Saunders SH, et al. 2021. Evidence of a streamlined extracellular electron transfer pathway from biofilm structure, metabolic stratification, and long-range electron transfer parameters. *Appl. Environ. Microbiol.* 87:e0070621
88. Chan CH, Levar CE, Jimenez-Otero F, Bond DR. 2017. Genome scale mutational analysis of *Geobacter sulfurreducens* reveals distinct molecular mechanisms for respiration and sensing of poised electrodes versus Fe(III) oxides. *J. Bacteriol.* 199:e00340-17
89. Howley E, Krajmalnik-Brown R, Torres CI. 2023. Cytochrome gene expression shifts in *Geobacter sulfurreducens* to maximize energy conservation in response to changes in redox conditions. *Biosens. Bioelectron.* 237:115524
90. Jahan MI, Juengwiwattanakitti P, Izu Y, Tobe R, Imai T, Mihara H. 2019. Selenite uptake by outer membrane porin ExtI and its involvement in the subcellular localization of rhodanese-like lipoprotein ExtH in *Geobacter sulfurreducens*. *Biochem. Biophys. Res. Commun.* 516:474–79
91. Jahan MI, Tobe R, Mihara H. 2018. Characterization of a novel porin-like protein, ExtI, from *Geobacter sulfurreducens* and its implication in the reduction of selenite and tellurite. *Int. J. Mol. Sci.* 19:809